Electronic Supplementary Material (ESI) for RSC Advances.

ELECTRONIC SUPPLEMENTARY INFORMATION

Effect of the substitution position (2, 3 or 8) on the spectroscopic and photophysical properties of BODIPY dyes with a phenyl, styryl or phenylethynyl group

Angel Orte,[†, a] Elke Debroye,[b] María J. Ruedas-Rama,[a] Emilio García Fernández,[a] David Robinson,[c] Luis Crovetto,[a] Eva M. Talavera,[a] Jose M. Alvarez-Pez,[a] Volker Leen,[b] Bram Verbelen,[b] Lucas Cunha Dias de Rezende,[b,d] Wim Dehaen,[b] Johan Hofkens,[b] Mark Van der Auweraer[b] and Noël Boens[†,b]

Table of Contents

Figures S1-S4. ^{1}H- and ^{13}C NMR spectra of **2-Styryl** and **8-Styryl** S2
Instability of 2-Styryl and 8-Styryl S6
Figures S5 and S6 S7
Table S1. Refractive index (n) and dielectric constant (ε) values of the solvents S8
Table S2. Spectroscopic and photophysical data of **8-Ethyn** S9
Figures S7-S9. Representative fluorescence decay traces S10
Details on the solvatochroism study S12
Tables S3-S6 S14
Figure S10. Correlations of fwhm$_{abs}$ and fwhm$_{em}$ *vs.* SdP S20
Figures S11-S14. Correlations of different parameters *vs.* ε and $f(n^2)$ S20
ESI References S22

---

[a] *Department of Physical Chemistry, Faculty of Pharmacy, University of Granada, Cartuja Campus, 18071 Granada, Spain.*
[b] *Department of Chemistry, KU Leuven (Katholieke Universiteit Leuven), Celestijnenlaan 200f, 3001 Leuven, Belgium.*
[c] *School of Chemistry, University Of Nottingham, University Park, Nottingham, NG7 2RD, United Kingdom.*
[d] *Faculdade de Ciências Farmacêuticas de Ribeirão Preto, Universidade de São Paulo, Av. Do Café s/n, Ribeirão Preto, SP, 14040-903, Brazil.*
† Corresponding authors: AO: E-mail: angelort@ugr.es, tel. +34-958243825. NB, E-mail: Noel.Boens@kuleuven.be

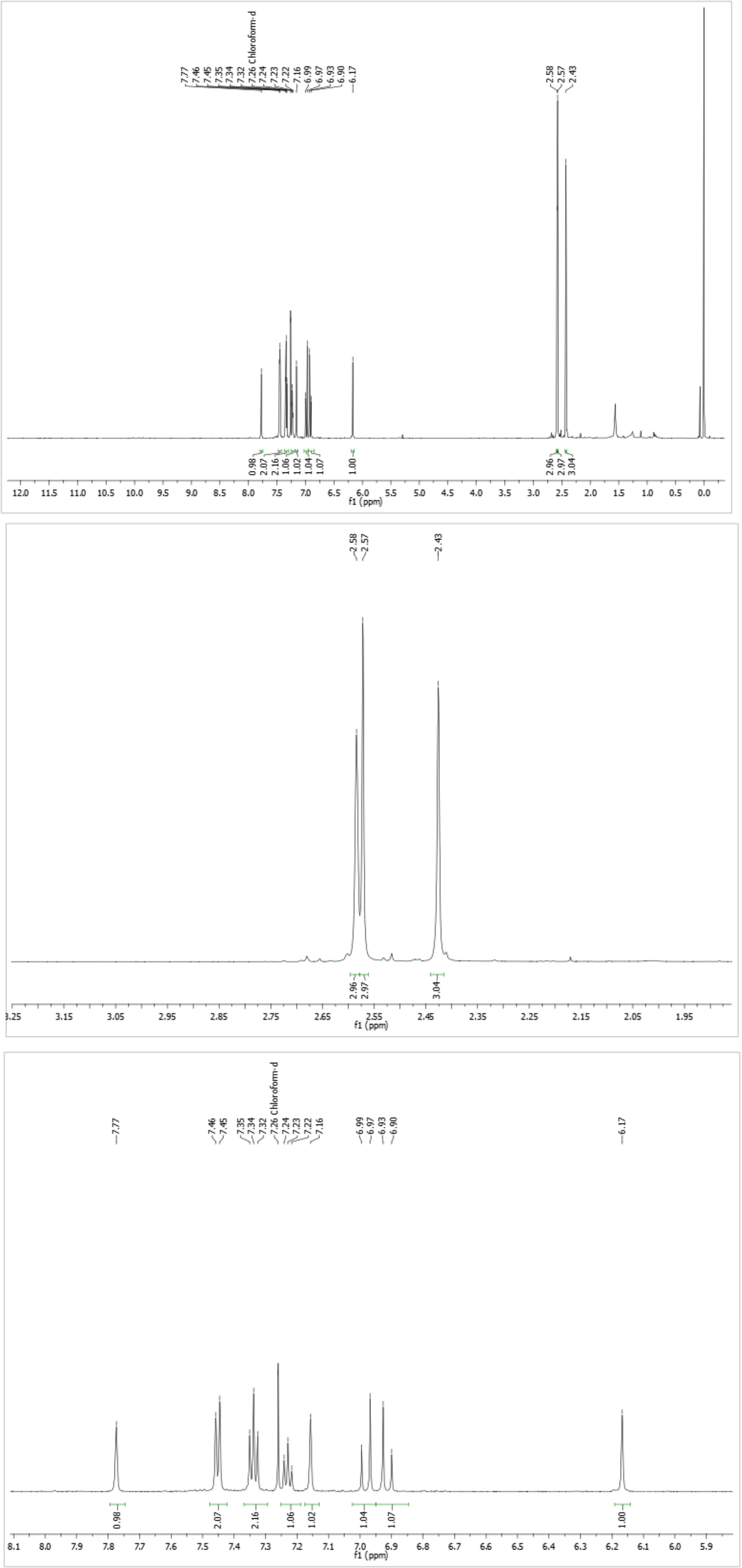

Figure S1. ^{1}H-NMR spectrum (600 MHz) of **2-Styryl** in $CDCl_3$.

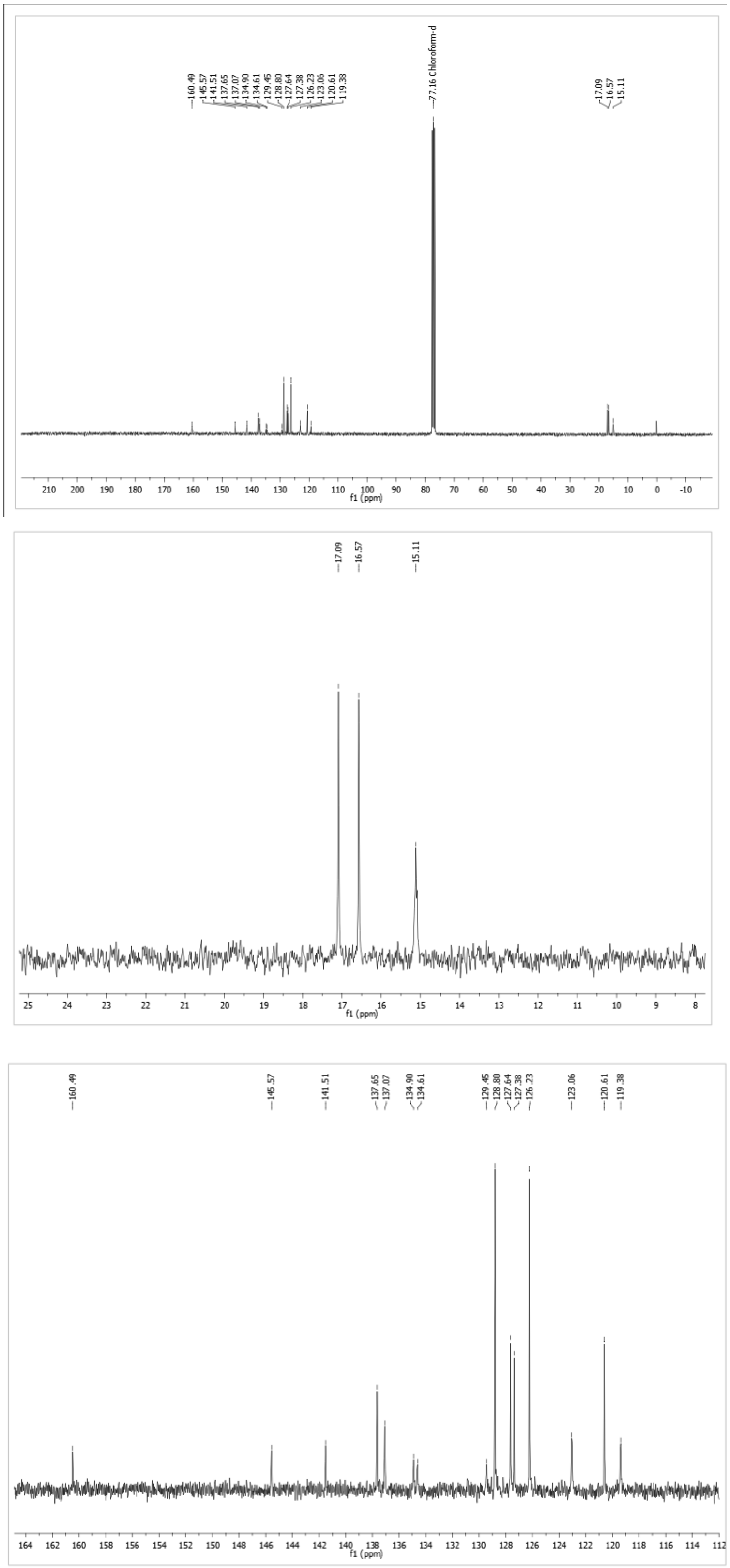

Figure S2. ^{13}C-NMR spectrum (600 MHz) of **2-Styryl** in CDCl$_3$.

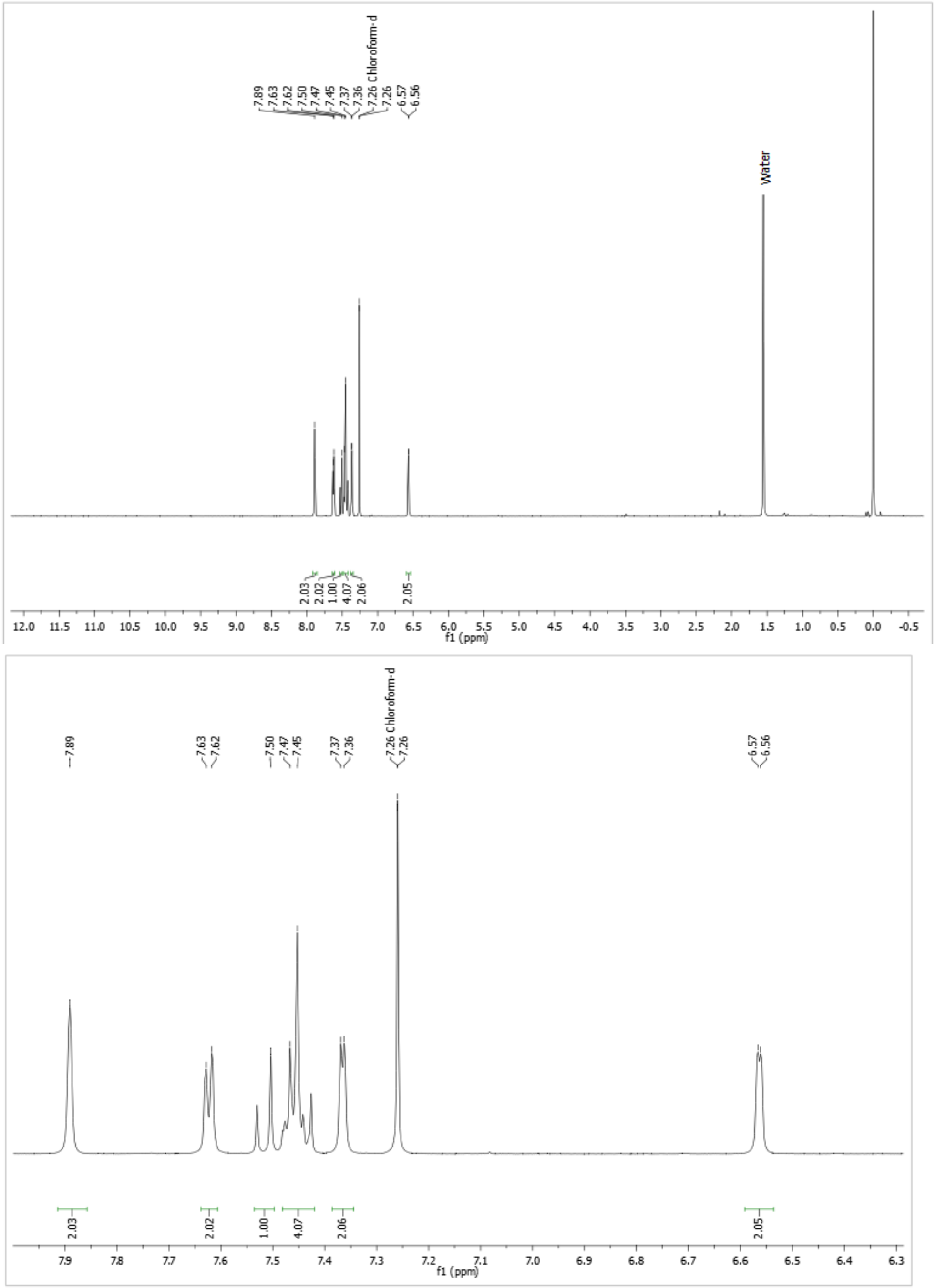

Figure S3. ^{1}H-NMR spectrum (600 MHz) of **8-Styryl** in $CDCl_3$.

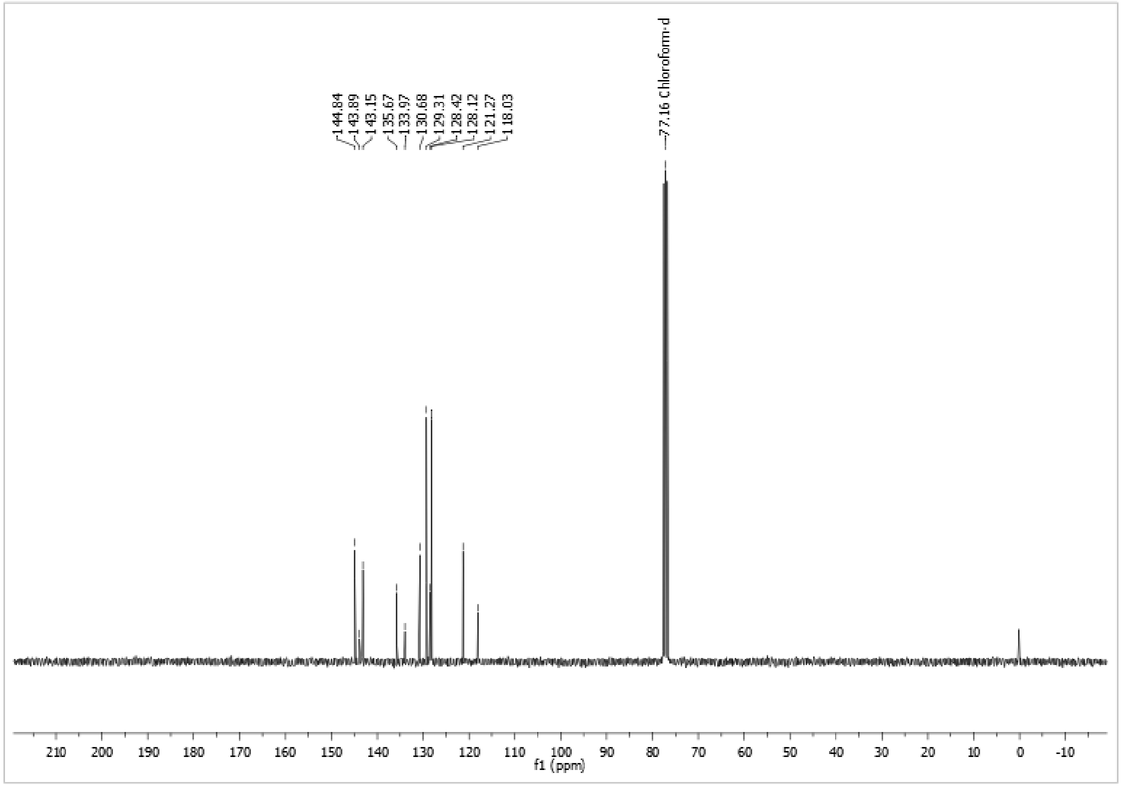

Figure S4. ^{13}C-NMR spectrum (75 MHz) of **8-Styryl** in $CDCl_3$.

Instability of 2-Styryl and 8-Styryl

The absorption and emission spectral features of the dyes **2-Styryl** and **8-Styryl** were not those typical for stable boron dipyrromethenes, such as the other dyes studied in this manuscript. For instance, both dyes exhibited very broad absorption spectra (black lines in Figs. S5A and S5B). But it is in the emission properties where the instable behavior was found more clearly. **2-Styryl** showed a dual excitation and emission behavior in acetone (Fig. S5A): a broad emission band with λ_{em}(max) = 599 nm, when excited at 530 nm; whereas a narrow emission band was found, with λ_{em}(max) = 499 nm, when excited at 480 nm. Likewise, two different excitation spectra were obtained when the emission was fixed at 510 nm or 610 nm (Fig. S5A, blue and cyan lines, respectively), neither of them matching the absorption spectrum. Time-resolved fluorescence measurements also provided intriguing results. When excited at 532 nm, and emission collected at 600 nm, bi-exponential decays were found with two lifetimes: τ_1 between 1.15 and 2.04 ns and τ_2 between 0.51 and 0.88 ns, depending on the solvent (acetone, acetonitrile, THF, CH_2Cl_2 and chlorobenzene). In contrast, a single exponential decay was found when excited at 485 nm and the emission collected at 500 nm, with a lifetime in the 4.57-5.76 ns range in the solvents tested (acetone, acetonitrile, THF, CH_2Cl_2 and chlorobenzene). Moreover, the fluorescence emission exhibited changes with time. The emission band of **2-Styryl** dissolved in cyclohexanone, when excited at 480 nm, increased with time (Fig. 6A), but the dye completely discolored after 48 h. When dissolved in THF, the emission was stable for 15 min, but the fluorescence emission disappeared completely after 180 min (Fig. S6B).

Regarding **8-Styryl**, the absorption spectrum exhibited two broad bands, but only the most red-shifted absorption band showed emission properties. The excitation spectrum (with λ_{em} = 540 nm) of **8-Styryl** did not match the absorption (Fig. S5B). The emission band in CH_2Cl_2 was centered at 530 nm, but clearly showed a shoulder at around 505 nm (red line in fig. S5B). This dual-band emission was also found in many other solvents. Finally, **8-Styryl** exhibited multi-exponential decay traces in the solvents tested (acetone, acetonitrile, THF, CH_2Cl_2 and chlorobenzene), and the relative contribution of each decay time varied at the different emission wavelengths tested (505 nm and 530 nm). This behavior clearly indicates the presence of different emissive species.

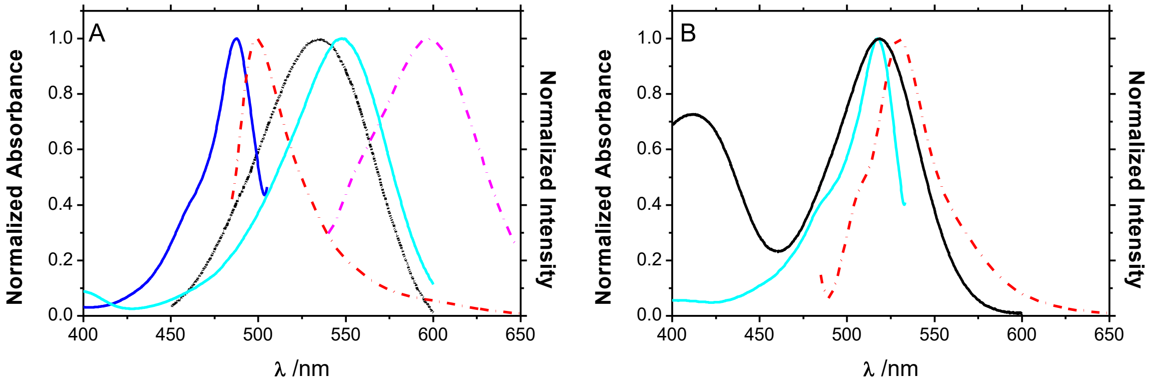

Figure S5: A) Normalized absorbance (black), fluorescence excitation (λ_{em} = 510 nm, blue; λ_{em} = 610 nm, cyan), and fluorescence emission spectra (λ_{ex} = 480 nm, dash-dotted red line; λ_{ex} = 530 nm, dash-dotted magenta line) of **2-Styryl** in acetone. B) Normalized absorbance (black), fluorescence excitation (λ_{em} = 540 nm, cyan), and fluorescence emission spectra (λ_{ex} = 480 nm, dash-dotted red line) of **8-Styryl** in CH_2Cl_2.

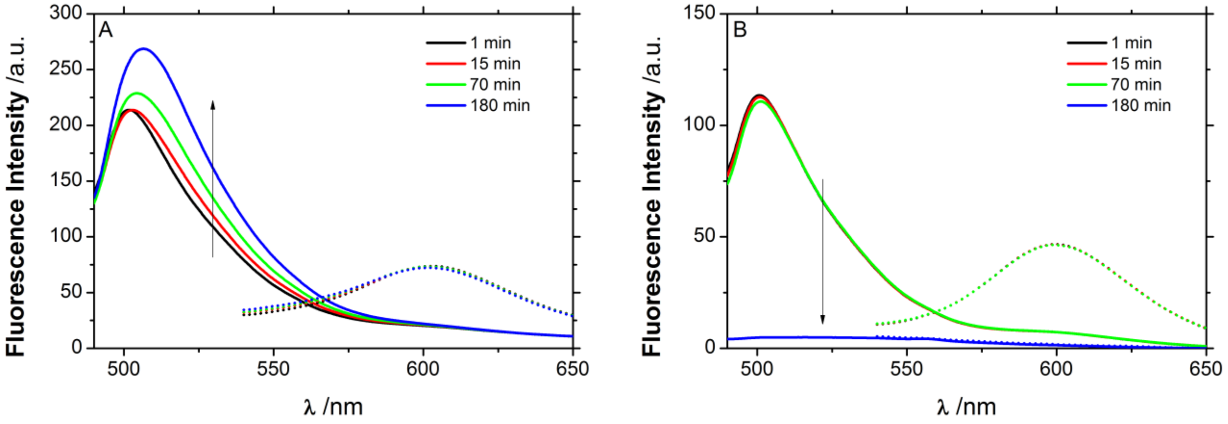

Figure S6. Time evolution of the fluorescence emission spectra of **2-Styryl** dissolved in cyclohexanone (A) and THF (B). λ_{ex} = 480 nm (solid lines) or 530 nm (dotted lines).

Table S1. Refractive index (n) dielectric constant (ε) values of the solvents used in this study.

	Solvent	n	ε
1	CH_3OH	1.3288	32.63
2	CH_3CN	1.3442	37.50
3	$(C_2H_5)_2O$	1.3526	4.335
4	Acetone	1.3588	20.70
5	EtOAc [a]	1.3723	6.02
6	2-Propanol	1.3776	18.30
7	PrCN [a]	1.3842	20.30
8	Bu_2O [a]	1.3992	3.06
9	THF [a]	1.4050	7.58
10	1-Pentanol	1.4101	13.9
11	1,4-Dioxane	1.4224	2.209
12	CH_2Cl_2	1.4242	9.08
13	c-C_6H_{12} [a]	1.4266	2.023
14	1-Octanol	1.4295	10.30
15	$CHCl_3$	1.4459	4.806
16	c-$C_6H_{10}O$ [a]	1.4507	18.30
17	Toluene	1.4961	2.438
18	PhCl [a]	1.5241	5.708

[a] EtOAc = ethyl acetate, PrCN = butanenitrile, Bu_2O = dibutyl ether, THF = tetrahydrofuran, c-C_6H_{12} = cyclohexane, c-$C_6H_{10}O$ = cyclohexanone, PhCl = chlorobenzene.

Table S2. Spectroscopic and photophysical data of **8-Ethyn** as a function of solvent. The solvents are numbered according to increasing refractive index *n*. (Data taken from *J. Phys. Chem. A* **2014**, *118*, 1576 –1594).[1]

Product		Solvent	λ_{abs}(max) [nm]	λ_{em}(max) [nm]	$\Delta \bar{\nu}$ [cm^{-1}]	fwhm$_{abs}$ [cm^{-1}]	fwhm$_{em}$ [cm^{-1}]	Φ [a]	τ [b] [ns]	k_f [c] [10^8 s^{-1}]	k_{nr} [c] [10^8 s^{-1}]
8-Ethyn	1	CH_3OH	539	553	470	975	1466	0.587± 0.006	7.16	0.82 ± 0.01	0.58 ± 0.01
	2	CH_3CN	537	553	539	1133	1551	0.624 ± 0.007	7.76	0.80 ± 0.01	0.48 ± 0.01
	3	$(C_2H_5)_2O$	541	555	466	879	1397	0.650 ± 0.004	7.80	0.83 ± 0.01	0.45 ± 0.01
	4	Acetone	539	554	502	1145	1539	0.55 ± 0.02	7.52	0.73 ± 0.03	0.60 ± 0.03
	5	EtOAc [d]	540	553	435	941	1443	0.65 ± 0.02	7.46	0.87 ± 0.03	0.47 ± 0.03
	6	Bu_2O [d]	543	556	431	837	1228	0.682 ± 0.005	7.21	0.95 ± 0.01	0.44 ± 0.01
	7	THF [d]	543	556	431	961	1426	0.632 ± 0.007	6.91	0.91 ± 0.01	0.53 ± 0.01
	8	1,4-Dioxane	544	558	461	921	1332	0.680 ± 0.005	6.92	0.98 ± 0.01	0.46 ± 0.01
	9	CH_2Cl_2	542	556	465	945	1339	0.658 ± 0.003	7.16	0.92 ± 0.01	0.48 ± 0.01
	10	$CHCl_3$	544	557	429	886	1206	0.686 ± 0.004	7.17	0.96 ± 0.01	0.44 ± 0.01
	11	Toluene	547	562	488	937	1380	0.715 ± 0.006	6.88	1.04 ± 0.01	0.41 ± 0.01
	12	PhCl [d]	547	561	456	911	1347	0.715 ± 0.005	6.72	1.06 ± 0.01	0.42 ± 0.01

[a] Fluorescence quantum yield ± one standard uncertainty. Φ determined *vs* rhodamine 6G in methanol (Φ_r = 0.86) as a reference.

[b] Fluorescence lifetime. The standard errors are obtained from the diagonal elements of the covariance matrix available from the global analysis fit of decay traces recorded at three emission wavelengths λ_{em} (555, 560, 565 nm) and are between 11 and 13 ps. λ_{ex} = 532 nm.

[c] The propagated errors are calculated using the uncertainty (standard deviation) of Φ and the standard error of τ.

[d] EtOAc = ethyl acetate, Bu_2O = dibutyl ether, THF = tetrahydrofuran, PhCl = chlorobenzene.

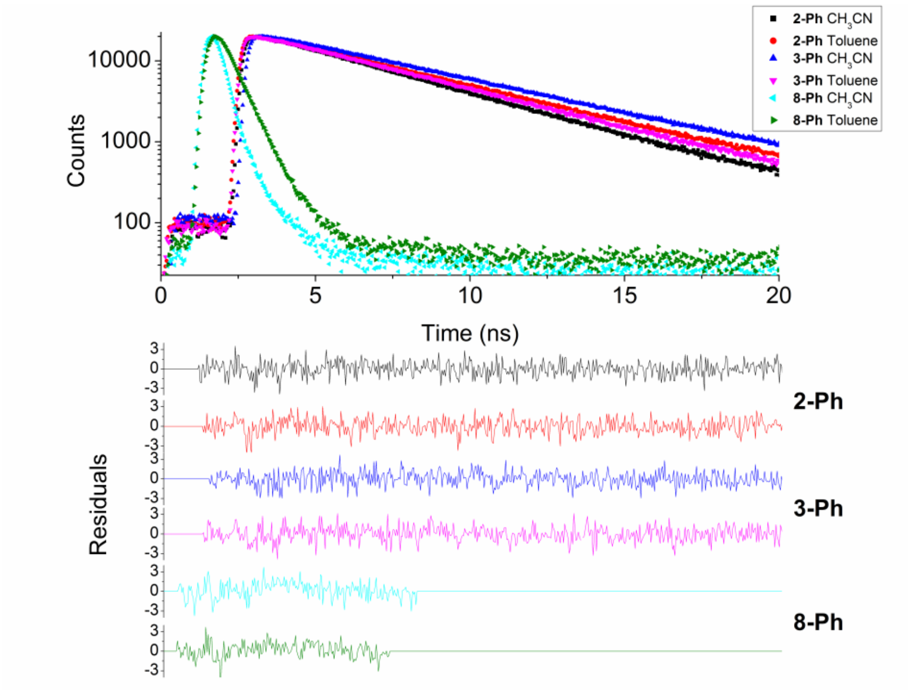

Figure S7. Fluorescence decay traces of **2-Ph**, **3-Ph** and **8-Ph** in acetonitrile and toluene. Weighted residuals from the single-exponential fits are shown below.

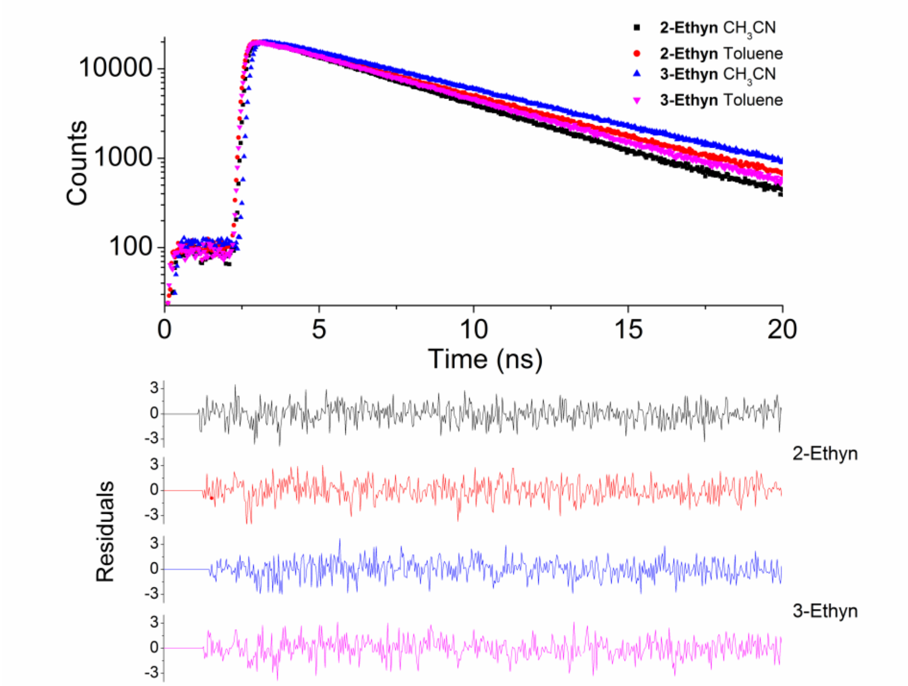

Figure S8. Fluorescence decay traces of **2-Ethyn** and **3-Ethyn** in acetonitrile and toluene. Weighted residuals from the single-exponential fits are shown below.

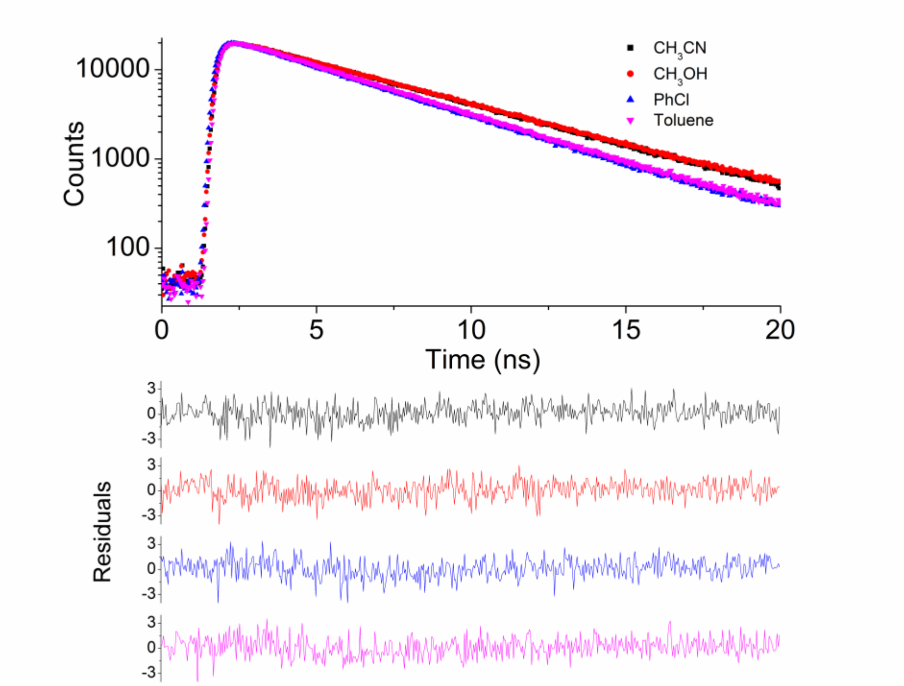

Figure S9. Fluorescence decay traces of **3-Styryl** in acetonitrile, methanol, chlorobenzene and toluene. Weighted residuals from the single-exponential fits are shown below.

Details on the solvatochroism study

The solvent effect on the physicochemical observable *y* is described by the multilinear eqn (2) (see main text), where y_0 denotes the physicochemical property of interest in the gas phase; a_{SA}, b_{SB}, c_{SP} and d_{SdP} are adjustable coefficients that reflect the dependency of the physicochemical property *y* in a given solvent on the {SA, SB, SP, SdP} solvent parameters. SA, SB, SP and SdP are four mutually independent, empirical solvent scales – introduced by Catalán[2] – that characterize respectively the solvent acidity, basicity, polarizability and dipolarity. The spectroscopic characteristics *y* analyzed are the absorption maxima $\bar{\nu}_{abs}$ [= $1/\lambda_{abs}$(max)] and the fluorescence emission maxima $\bar{\nu}_{em}$ [= $1/\lambda_{em}$(max)], both expressed in cm^{-1}, and the S_1 deactivation rate constants k_f and k_{nr} (see main text). The values of {SA, SB, SP, SdP} for an extensive list of solvents can be found in ref [2].

The distinctive advantage of the generalized (i.e., Catalán) treatment of the solvent effect over all the other approaches is that it allows one to disentangle the relative contributions of dipolarity, polarizability, acidity and basicity of the medium. Hence, it is instructive to determine by the Catalán approach the solvent properties that contribute primarily to the observed solvatochromic shifts of $\bar{\nu}_{abs}$ and $\bar{\nu}_{em}$, and the solvent-dependent changes of k_f and k_{nr} (see main text).

Here we shall discuss in detail the solvatochromic analyses of $\bar{\nu}_{abs}$ and $\bar{\nu}_{em}$ of **3-Ethyn** only. The high-quality fit (r = 0.933) of $y = \bar{\nu}_{abs}$ of **3-Ethyn** according to eqn (2) with {SA, SB, SP, SdP} as independent variables yields large c_{SP} and d_{SdP} estimates with high precision (*i.e.*, comparatively small standard error) in relation to the small a_{SA} and b_{SB} estimates with relatively high standard errors (Table S3). This is indicative that the change of $\bar{\nu}_{abs}$ reflects predominantly a change in polarizability and dipolarity of the environment of the dye. If either SP or SdP was left out as independent variable in the analyses of $y = \bar{\nu}_{abs}$ of **3-Ethyn** according to eqn (2), relatively low r-values were found (0.850 for {SA, SB, SdP} and 0.522 for {SA, SB, SP}), implying the importance of these solvent parameters, especially of SdP. Conversely, the two analyses of $y = \bar{\nu}_{abs}$ according to eqn (2) in which both SP and SdP are present as independent variables (i.e., with {SA, SP, SdP} and {SB, SP, SdP}), gave high-quality fits (r = 0.933 and 0.900, respectively). Further corroboration for SP and SdP as major factors came from the six analyses with two solvent scales as independent variables: the analysis with {SP, SdP} yielded the highest r-value (0.893). In contrast, an unacceptable fit (r = 0.178) was found for the analysis with {SA, SB} as independent variables, confirming that solvent acidity and basicity have a negligible effect on $\bar{\nu}_{abs}$.

The Catalán {SA, SB, SP, SdP} solvent scales [eqn (2)] also describe excellently the solvatochromic shifts of $\bar{\nu}_{em}$ (r = 0.922, Table S3). The large negative c_{SP} and positive d_{SdP} estimates with comparatively small standard errors in relation to the smaller a_{SA} and b_{SB} estimates with relatively high standard errors (Table S3) show that the shifts of $\bar{\nu}_{em}$ reflect primarily a change in polarizability and dipolarity of the environment surrounding the dye. To confirm this, we performed – as for $\bar{\nu}_{abs}$ – some additional regression analyses of $y = \bar{\nu}_{em}$ according to eqn (2) in which systematically one or two solvent scales were omitted. These analogous analyses of $\overline{\nu}_{em}$ of **3-Ethyn** corroborated that solvent polarizability and dipolarity are the key factors determining the position of $\overline{\nu}_{em}$. For instance – as for $\overline{\nu}_{abs}$ – the analyses of $\overline{\nu}_{em}$ in which one solvent scale was omitted clearly identify solvent polarizability and dipolarity as the most critical for $\overline{\nu}_{em}$ (see Table S3). Indeed, as long as both {SP, SdP} are present in the analyses of $y = \overline{\nu}_{em}$ according to eqn (2), good fits are obtained ($r = 0.918$ for {SA, SP, SdP} and 0.881 for {SB, SP, SdP}, Table S3). In contrast, the two analysis of $y = \overline{\nu}_{em}$ according to eqn (2), in which either solvent polarizability or dipolarity was disregarded, produced lower *r*-values ($r = 0.637$ for {SA, SB, SdP} and 0.764 for {SA, SB, SdP}, Table S3). Hence, as found for $\overline{\nu}_{abs}$, solvent polarizability and dipolarity are the most important solvent properties determining the position of $\overline{\nu}_{em}$. This was confirmed further by the good regression according to eqn (2) of $y = \overline{\nu}_{em}$ vs {SP, SdP} ($r = 0.855$) and the unacceptable fit *vs* {SA, SB} ($r = 0.187$).

Similar analyses of $y = \overline{\nu}_{abs}$ and $y = \overline{\nu}_{em}$ of **2-Ethyn** and **8-Ethyn** (Table S3), **3-Ph**, **2-Ph** and **8-Ph** (Table S4), and **3-Styryl** (Table S5) according to eqn (2) showed that solvent polarizability and dipolarity are the major causes for the solvatochromic shifts of the absorption ($\overline{\nu}_{abs}$) and fluorescence emission ($\overline{\nu}_{em}$) maxima.

Table S3. Estimated coefficients [y_0, a_{SA}, b_{SB}, c_{SP}, d_{SdP}: eqn (2)], their standard errors and correlation coefficients (r) for the multilinear regression analyses of $\bar{\nu}_{\mathrm{abs}}$ and $\bar{\nu}_{\mathrm{em}}$ of **3-Ethyn**, **2-Ethyn** and **8-Ethyn** (next page) for the solvents listed in Table S1 as a function of {SA, SB, SP, SdP}. The estimates are expressed in cm^{-1}.

		y_0	a_{SA}	b_{SB}	c_{SP}	d_{SdP}	r
3-Ethyn	$\bar{\nu}_{\mathrm{abs}}$	$(19.3 \pm 0.3) \times 10^3$	–327 ± 133	–6 ± 88	–1318 ± 342	551 ± 71	0.933
	$\bar{\nu}_{\mathrm{abs}}$	$(19.3 \pm 0.3) \times 10^3$		–93 ± 94	–1192 ± 95	508 ± 81	0.900
	$\bar{\nu}_{\mathrm{abs}}$	$(19.3 \pm 0.2) \times 10^3$	–331 ± 117		–1309 ± 305	552 ± 69	0.933
	$\bar{\nu}_{\mathrm{abs}}$	$(18.3 \pm 0.1) \times 10^3$	–250 ± 185	122 ± 115		588 ± 100	0.850
	$\bar{\nu}_{\mathrm{abs}}$	$(19.9 \pm 0.6) \times 10^3$	–70 ± 293	–57 ± 200	–1668 ± 774		0.522
	$\bar{\nu}_{\mathrm{abs}}$	$(19.1 \pm 0.3) \times 10^3$			–1003 ± 345	505 ± 80	0.893
	$\bar{\nu}_{\mathrm{abs}}$	$(18.6 \pm 0.1) \times 10^3$	51 ± 321	105 ± 207			0.178
	$\bar{\nu}_{\mathrm{em}}$	$(18.9 \pm 0.2) \times 10^3$	–201 ± 80	–43 ± 53	–1277 ± 207	206 ± 43	0.922
	$\bar{\nu}_{\mathrm{em}}$	$(18.9 \pm 0.2) \times 10^3$		–96 ± 57	–1199 ± 240	179 ± 49	0.881
	$\bar{\nu}_{\mathrm{em}}$	$(18.9 \pm 0.1) \times 10^3$	–227 ± 73		–1214 ± 189	209 ± 42	0.918
	$\bar{\nu}_{\mathrm{em}}$	$(18.0 \pm 0.1) \times 10^3$	–127 ± 152	84 ± 94		241 ± 82	0.637
	$\bar{\nu}_{\mathrm{em}}$	$(19.1 \pm 0.2) \times 10^3$	–105 ± 124	–62 ± 85	–1408 ± 328		0.764
	$\bar{\nu}_{\mathrm{em}}$	$(18.7 \pm 0.2) \times 10^3$			–1003 ± 222	177 ± 52	0.855
	$\bar{\nu}_{\mathrm{em}}$	$(18.1 \pm 0.1) \times 10^3$	–3 ± 179	74 ± 116			0.187
2-Ethyn	$\bar{\nu}_{\mathrm{abs}}$	$(19.8 \pm 0.3) \times 10^3$	–393 ± 162	41 ± 108	–1089 ± 418	708 ± 87	0.930
	$\bar{\nu}_{\mathrm{abs}}$	$(19.8 \pm 0.4) \times 10^3$		–63 ± 114	–938 ± 480	655 ± 98	0.896
	$\bar{\nu}_{\mathrm{abs}}$	$(19.9 \pm 0.3) \times 10^3$	–368 ± 144		–1150 ± 375	705 ± 84	0.929
	$\bar{\nu}_{\mathrm{abs}}$	$(19.0 \pm 0.1) \times 10^3$	–330 ± 191	147 ± 118		737 ± 103	0.891
	$\bar{\nu}_{\mathrm{abs}}$	$(20.6 \pm 0.7) \times 10^3$	–63 ± 373	24 ± –255	–1538 ± 985		0.416
	$\bar{\nu}_{\mathrm{abs}}$	$(19.6 \pm 0.3) \times 10^3$			–809 ± 410	653 ± 96	0.894
	$\bar{\nu}_{\mathrm{abs}}$	$(19.4 \pm 0.1) \times 10^3$	48 ± 384	125 ± 247			0.172
	$\bar{\nu}_{\mathrm{em}}$	$(18.4 \pm 0.2) \times 10^3$	–90 ± 74	–49 ± 49	–659 ± 192	–356 ± 40	0.939
	$\bar{\nu}_{\mathrm{em}}$	$(18.4 \pm 0.2) \times 10^3$		–73 ± 46	–624 ± 193	–369 ± 39	0.932
	$\bar{\nu}_{\mathrm{em}}$	$(18.4 \pm 0.1) \times 10^3$	–120 ± 68		–587 ± 177	–353 ± 40	0.934
	$\bar{\nu}_{\mathrm{em}}$	$(17.9 \pm 0.1) \times 10^3$	–52 ± 98	15 ± 61		–338 ± 53	0.880
	$\bar{\nu}_{\mathrm{em}}$	$(18.1 \pm 0.4) \times 10^3$	–257 ± 185	–16 ± 127	–433 ± 489		0.393
	$\bar{\nu}_{\mathrm{em}}$	$(18.3 \pm 0.1) \times 10^3$			–475 ± 177	–370± 41	0.919
	$\bar{\nu}_{\mathrm{em}}$	$(17.7 \pm 0.1) \times 10^3$	–225 ± 181	26 ± 116			0.327

		y_0	a_{SA}	b_{SB}	c_{SP}	d_{SdP}	r
8-Ethyn	$\bar{\nu}_{\mathrm{abs}}$	$(19.2 \pm 0.2) \times 10^3$	–112 ± 55	–68 ± 72	–1253 ± 211	197 ± 40	0.979
	$\bar{\nu}_{\mathrm{abs}}$	$(19.2 \pm 0.2) \times 10^3$		–65 ± 85	–1170 ± 245	173 ± 45	0.967
	$\bar{\nu}_{\mathrm{abs}}$	$(19.1 \pm 0.1) \times 10^3$	–112 ± 55		–1090 ± 122	217 ± 34	0.977
	$\bar{\nu}_{\mathrm{abs}}$	$(18.2 \pm 0.1) \times 10^3$	–50 ± 124	278 ± 95		315 ± 80	0.867
	$\bar{\nu}_{\mathrm{abs}}$	$(19.8 \pm 0.3) \times 10^3$	–33 ± 104	–245 ± 122	–1768 ± 362		0.904
	$\bar{\nu}_{\mathrm{abs}}$	$(19.0 \pm 0.1) \times 10^3$			–1014 ± 134	192 ± 37	0.964
	$\bar{\nu}_{\mathrm{abs}}$	$(18.4 \pm 0.1) \times 10^3$	173 ± 179	203 ± 151			0.518
	$\bar{\nu}_{\mathrm{em}}$	$(18.4 \pm 0.3) \times 10^3$	–68 ± 88	70 ± 114	–837 ± 337	170 ± 64	0.933
	$\bar{\nu}_{\mathrm{em}}$	$(18.4 \pm 0.3) \times 10^3$		72 ± 111	–787 ± 323	156 ± 60	0.927
	$\bar{\nu}_{\mathrm{em}}$	$(18.6 \pm 0.1) \times 10^3$	–69 ± 85		–1006 ± 188	150 ± 53	0.929
	$\bar{\nu}_{\mathrm{em}}$	$(17.7 \pm 0.1) \times 10^3$	–26 ± 111	302 ± 85		249 ± 71	0.870
	$\bar{\nu}_{\mathrm{em}}$	$(18.9 \pm 0.3) \times 10^3$	0 ± 122	–83 ± 131	–1281 ± 388		0.860
	$\bar{\nu}_{\mathrm{em}}$	$(18.6 \pm 0.1) \times 10^3$			–959 ± 175	135 ± 49	0.923
	$\bar{\nu}_{\mathrm{em}}$	$(17.9 \pm 0.1) \times 10^3$	150 ± 148	243 ± 125			0.622

Table S4. Estimated coefficients [y_0, a_{SA}, b_{SB}, c_{SP}, d_{SdP}: eqn (2)], their standard errors and correlation coefficients (r) for the multilinear regression analyses of $\bar{\nu}_{abs}$ and $\bar{\nu}_{em}$ of **3-Ph**, **2-Ph** and **8-Ph** (next page) for the solvents listed in Tables 1 and 2 as a function of {SA, SB, SP, SdP}. The estimates are expressed in cm^{-1}.

		y_0	a_{SA}	b_{SB}	c_{SP}	d_{SdP}	r
3-Ph	$\bar{\nu}_{abs}$	(19.9 ± 0.2) × 10^3	–147 ± 105	–71 ± 70	–1252 ± 271	379 ± 56	0.928
	$\bar{\nu}_{abs}$	(19.9 ± 0.2) × 10^3		–110 ± 66	–1196 ± 277	359 ± 56	0.916
	$\bar{\nu}_{abs}$	(19.8 ± 0.2) × 10^3	–190 ± 97		–1147 ± 251	383 ± 56	0.921
	$\bar{\nu}_{abs}$	(18.9 ± 0.1) × 10^3	–74 ± 163	51 ± 101		413 ± 88	0.795
	$\bar{\nu}_{abs}$	(20.3 ± 0.4) × 10^3	30 ± 207	–106 ± 142	–1492 ± 547		0.613
	$\bar{\nu}_{abs}$	(19.6 ± 0.2) × 10^3			–971 ± 256	356 ± 60	0.899
	$\bar{\nu}_{abs}$	(19.1 ± 0.1) × 10^3	138 ± 243	38 ± 157			0.212
	$\bar{\nu}_{em}$	(19.0 ± 0.1) × 10^3	–157 ± 68	–57 ± 45	–1202 ± 176	162 ± 37	0.926
	$\bar{\nu}_{em}$	(18.9 ± 0.2) × 10^3		–98 ± 47	–1142 ± 199	141 ± 41	0.894
	$\bar{\nu}_{em}$	(18.9 ± 0.1) × 10^3	–191 ± 64		–1119 ± 166	166 ± 37	0.917
	$\bar{\nu}_{em}$	(18.0 ± 0.1) × 10^3	–87 ± 139	61 ± 86		195 ± 75	0.589
	$\bar{\nu}_{em}$	(19.1 ± 0.2) × 10^3	–82 ± 101	–71 ± 69	–1305 ± 266		0.802
	$\bar{\nu}_{em}$	(18.8 ± 0.1) × 10^3			–942 ± 192	139 ± 45	0.859
	$\bar{\nu}_{em}$	(18.2 ± 0.1) × 10^3	13 ± 158	55 ± 102			0.173
2-Ph	$\bar{\nu}_{abs}$	(19.8 ± 0.2) × 10^3	–131 ± 93	–77 ± 62	–1228 ± 241	381 ± 50	0.942
	$\bar{\nu}_{abs}$	(19.8 ± 0.2) × 10^3		–111 ± 59	–1178 ± 246	364 ± 50	0.932
	$\bar{\nu}_{abs}$	(19.7 ± 0.2) × 10^3	–178 ± 87		–1115 ± 227	386 ± 51	0.935
	$\bar{\nu}_{abs}$	(18.8 ± 0.1) × 10^3	–60 ± 154	43 ± 96		415 ± 83	0.812
	$\bar{\nu}_{abs}$	(20.2 ± 0.4) × 10^3	46 ± 203	–112 ± 139	–1470 ± 537		0.617
	$\bar{\nu}_{abs}$	(19.5 ± 0.2) × 10^3			–951 ± 233	361 ± 54	0.914
	$\bar{\nu}_{abs}$	(19.1 ± 0.1) × 10^3	152 ± 239	31 ± 154			0.223
	$\bar{\nu}_{em}$	(18.4 ± 0.1) × 10^3	–30 ± 53	–161 ± 35	–1037 ± 137	–482 ± 29	0.982
	$\bar{\nu}_{em}$	(18.4 ± 0.1) × 10^3		–169 ± 31	–1026 ± 132	–487 ± 27	0.981
	$\bar{\nu}_{em}$	(18.1 ± 0.1) × 10^3	–128 ± 76		–799 ± 197	–473 ± 44	0.952
	$\bar{\nu}_{em}$	(17.6 ± 0.1) × 10^3	30 ± 118	–60 ± 73		–454 ± 63	0.897
	$\bar{\nu}_{em}$	(17.9 ± 0.5) × 10^3	–255 ± 238	–117 ± 162	–731 ± 628		0.413
	$\bar{\nu}_{em}$	(18.1 ± 0.1) × 10^3			–681 ± 195	–491 ± 46	0.942
	$\bar{\nu}_{em}$	(17.3 ± 0.1) × 10^3	–202 ± 236	–46 ± 152			0.300

		y_0	a_{SA}	b_{SB}	c_{SP}	d_{SdP}	r
8-Ph	$\overline{\nu}_{\mathrm{abs}}$	$(21.0 \pm 0.1) \times 10^3$	−101 ± 55	−35 ± 36	−1151 ± 141	205 ± 29	0.959
	$\overline{\nu}_{\mathrm{abs}}$	$(21.0 \pm 0.1) \times 10^3$		−61 ± 36	−1111 ± 151	192 ± 31	0.948
	$\overline{\nu}_{\mathrm{abs}}$	$(20.9 \pm 0.1) \times 10^3$	−122 ± 50		−1100 ± 130	208 ± 29	0.956
	$\overline{\nu}_{\mathrm{abs}}$	$(20.1 \pm 0.1) \times 10^3$	−35 ± 129	78 ± 80		237 ± 69	0.711
	$\overline{\nu}_{\mathrm{abs}}$	$(21.2 \pm 0.2) \times 10^3$	−6 ± 111	−53 ± 76	−1281 ± 294		0.784
	$\overline{\nu}_{\mathrm{abs}}$	$(20.9 \pm 0.1) \times 10^3$			−986 ± 140	190 ± 33	0.936
	$\overline{\nu}_{\mathrm{abs}}$	$(20.2 \pm 0.1) \times 10^3$	87 ± 162	71 ± 105			0.302
	$\overline{\nu}_{\mathrm{em}}$	$(19.8 \pm 0.2) \times 10^3$	−62 ± 115	122 ± 76	−671 ± 297	211 ± 62	0.844
	$\overline{\nu}_{\mathrm{em}}$	$(19.8 \pm 0.2) \times 10^3$		105 ± 68	−647 ± 286	203 ± 58	0.840
	$\overline{\nu}_{\mathrm{em}}$	$(20.0 \pm 0.2) \times 10^3$	12 ± 111		−851 ± 289	204 ± 65	0.810
	$\overline{\nu}_{\mathrm{em}}$	$(19.3 \pm 0.1) \times 10^3$	−23 ± 129	187 ± 80		230 ± 70	0.774
	$\overline{\nu}_{\mathrm{em}}$	$(20.0 \pm 0.3) \times 10^3$	37 ± 148	102 ± 101	−805 ± 391		0.673
	$\overline{\nu}_{\mathrm{em}}$	$(20.0 \pm 0.2) \times 10^3$			−862 ± 261	206 ± 61	0.810
	$\overline{\nu}_{\mathrm{em}}$	$(19.5 \pm 0.1) \times 10^3$	95 ± 160	180 ± 103			0.535

Table S5. Estimated coefficients [y_0, a_{SA}, b_{SB}, c_{SP}, d_{SdP}: eqn (2)], their standard errors and correlation coefficients (r) for the multilinear regression analyses of $\bar{\nu}_{\mathrm{abs}}$ and $\bar{\nu}_{\mathrm{em}}$ of **3-Styryl** for the solvents listed in Table 4 as a function of {SA, SB, SP, SdP}. The estimates are expressed in cm^{-1}.

		y_0	a_{SA}	b_{SB}	c_{SP}	d_{SdP}	r
3-Styryl	$\bar{\nu}_{\mathrm{abs}}$	$(18.9 \pm 0.2) \times 10^3$	–165 ± 81	–33 ± 57	–1450 ± 217	222 ± 46	0.938
	$\bar{\nu}_{\mathrm{abs}}$	$(18.9 \pm 0.2) \times 10^3$		–70 ± 60	–1363 ± 237	192 ± 48	0.915
	$\bar{\nu}_{\mathrm{abs}}$	$(18.9 \pm 0.1) \times 10^3$	–180 ± 75		–1393 ± 188	221 ± 45	0.936
	$\bar{\nu}_{\mathrm{abs}}$	$(17.8 \pm 0.1) \times 10^3$	–59 ± 166	140 ± 106		231 ± 96	0.655
	$\bar{\nu}_{\mathrm{abs}}$	$(19.1 \pm 0.3) \times 10^3$	–38 ± 127	–27 ± 94	–1480 ± 358		0.802
	$\bar{\nu}_{\mathrm{abs}}$	$(18.8 \pm 0.1) \times 10^3$			–1210 ± 200	184 ± 48	0.906
	$\bar{\nu}_{\mathrm{abs}}$	$(17.9 \pm 0.1) \times 10^3$	75 ± 181	151 ± 123			0.417
	$\bar{\nu}_{\mathrm{em}}$	$(18.8 \pm 0.1) \times 10^3$	–166 ± 71	–63 ± 50	–1567 ± 190	132 ± 40	0.942
	$\bar{\nu}_{\mathrm{em}}$	$(18.7 \pm 0.2) \times 10^3$		–101 ± 55	–1480 ± 216	101 ± 44	0.914
	$\bar{\nu}_{\mathrm{em}}$	$(18.7 \pm 0.1) \times 10^3$	–195 ± 69		–1458 ± 174	131 ± 41	0.934
	$\bar{\nu}_{\mathrm{em}}$	$(17.6 \pm 0.1) \times 10^3$	–52 ± 173	124 ± 111		141 ± 100	0.496
	$\bar{\nu}_{\mathrm{em}}$	$(18.9 \pm 0.2) \times 10^3$	–91 ± 89	–59 ± 66	–1585 ± 252		0.886
	$\bar{\nu}_{\mathrm{em}}$	$(18.6 \pm 0.1) \times 10^3$			–1261 ± 195	90 ± 47	0.890
	$\bar{\nu}_{\mathrm{em}}$	$(17.7 \pm 0.1) \times 10^3$	31 ± 169	130 ± 115			0.359

Table S6. Estimated coefficients [y_0, a_SA, b_SB, c_SP, d_SdP: eqn (2); y_0, a: eqn (3); y_0, b: eqn (4)], their standard errors and correlation coefficients (r) for the (multi)linear regression analyses of k_f and k_nr of **3-Ph**, **2-Ph**, **8-Ph**, **3-Ethyn**, **2-Ethyn**, **8-Ethyn** and **3-Styryl** for the solvents listed in Table S1 as a function of {SA, SB, SP, SdP} [eqn (2)], ε [eqn (3)] or $f(n^2)$ [eqn (4)]. The fitting eqns (2), (3) and (4) are given in the main text. All estimates are expressed in 10^8 s^{-1}.

		y_0	a_SA or a	b_SB or b	c_SP	d_SdP	r	*Fitting eqn*
3-Ph	k_f	1.2 ± 0.4	–0.3 ± 0.2	0.1 ± 0.1	1.3 ± 0.5	–0.3 ± 0.1	0.816	(2)
2-Ph	k_nr	0.7 ± 0.6	0.5 ± 0.3	–0.2 ± 0.2	–0.2 ± 0.7	0.6 ± 0.2	0.813	(2)
	k_nr	0.48 ± 0.09	–	–	–	0.7 ± 0.1	0.766	(2)
	k_nr	0.65 ± 0.05	0.019 ± 0.003				0.827	(3)
	k_nr	2.1 ± 0.6		–6 ± 3			0.439	(4)
8-Ph	k_nr	139 ± 18	–19 ± 9	–13 ± 6	–157 ± 23	20 ± 5	0.924	(2)
	k_nr	125 ± 22	–	–	–130 ± 31	–	0.722	(2)
	k_nr	24 ± 3	0.7 ± 0.2				0.677	(3)
	k_nr	143 ± 19		–554 ± 94			0.829	(4)
3-Ethyn	k_f	1.1 ± 0.4	0.2 ± 0.2	–0.2 ± 0.1	1.5 ± 0.5	–0.4 ± 0.1	0.847	(2)
	k_nr	–0.04 ± 0.4	–0.2 ± 0.2	0.2 ± 0.1	0.01 ± 0.5	0.3 ± 0.1	0.710	(2)
2-Ethyn	k_nr	0.8 ± 0.9	0.1 ± 0.5	–0.2 ± 0.3	–0.4 ± 1.2	1.1 ± 0.3	0.802	(2)
	k_nr	0.4 ± 0.1	–	–	–	1.1 ± 0.2	0.797	(2)
	k_nr	0.71 ± 0.08	0.031 ± 0.005				0.827	(3)
	k_nr	3 ± 1		–9 ± 5			0.403	(4)
8-Ethyn	k_f	0.2 ± 0.2	0.15 ± 0.06	0.02 ± 0.07	1.1 ± 0.2	–0.20 ± 0.04	0.975	(2)
	k_f	0.3 ± 0.1	–	–	1.0 ± 0.1	–0.17 ± 0.04	0.950	(2)
	k_f	0.03 ± 0.12		4.5 ± 0.6			0.915	(4)
	k_nr	0.1 ± 0.2	0.05 ± 0.07	0.21 ± 0.09	0.2 ± 0.3	0.18 ± 0.05	0.899	(2)
3-Styryl	k_nr	–0.6 ± 0.4	0.08 ± 0.20	0.3 ± 0.1	2.4 ± 0.5	–0.2 ± 0.1	0.831	(2)
	k_nr	1.11 ± 0.06	–0.005 ± 0.004				0.328	(3)
	k_nr	–0.5 ± 0.3		8 ± 2			0.804	(4)

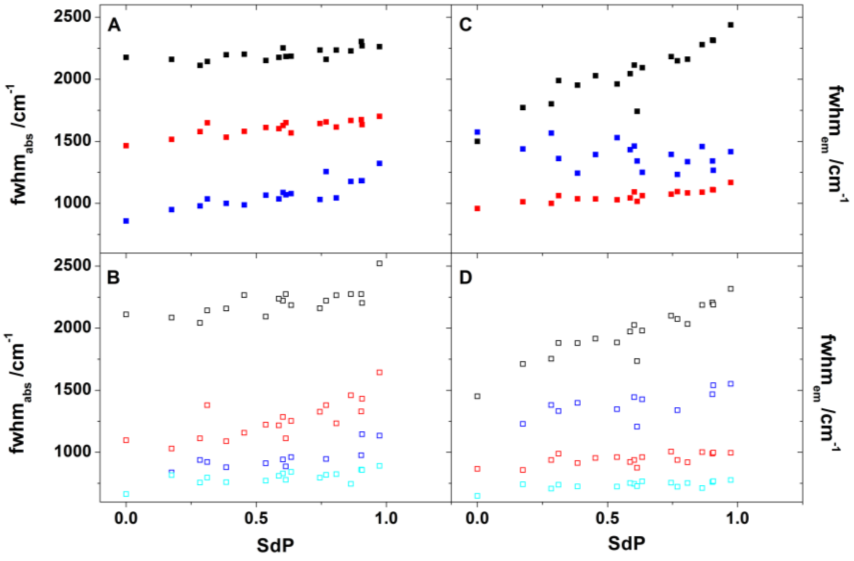

Figure S10. Correlations of fwhm$_{abs}$ (A and B) and fwhm$_{em}$ (C and D) *vs.* the Catalán dipolarity parameter, SdP, for the BODIPY derivatives **2-Ph** (■), **3-Ph** (🟥), **8-Ph** (🟦), **2-Ethyn** (□), **3-Ethyn** (□), **8-Ethyn** (□), and **3-Styryl** (□).

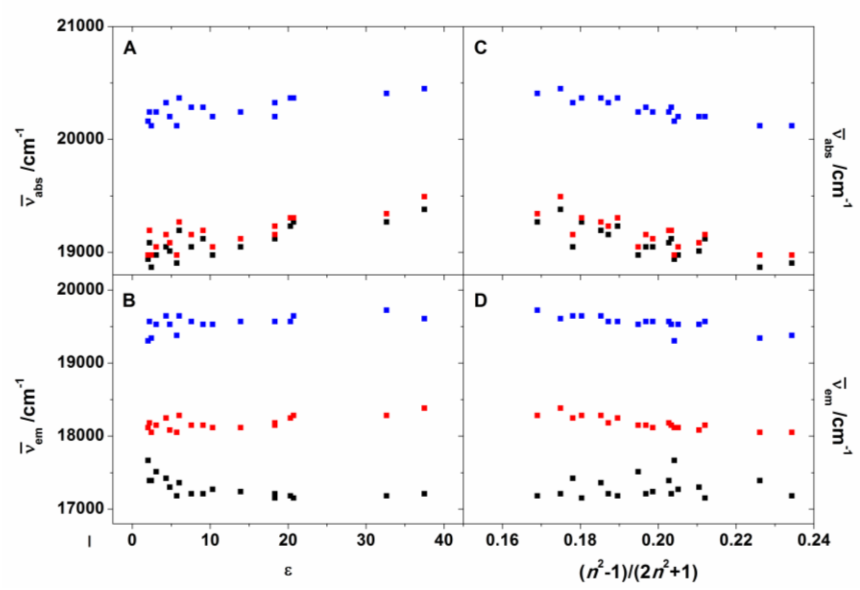

Figure S11. Correlations of $\bar{\nu}_{abs}$ and $\bar{\nu}_{em}$ *vs.* the dielectric constant, ε (A and B), and $f(n^2)$ (C and D) for the BODIPY derivatives **2-Ph** (■), **3-Ph** (🟥), and **8-Ph** (🟦).

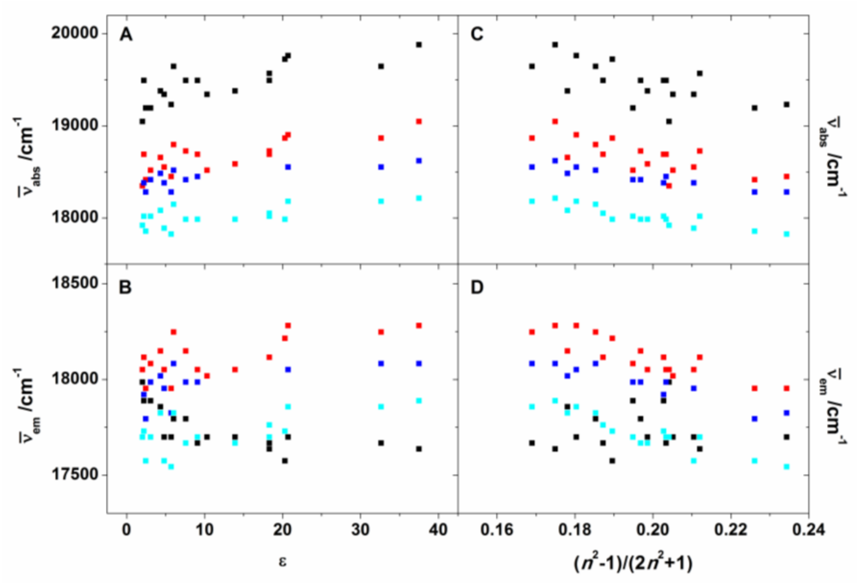

Figure S12. Correlations of $\bar{\nu}_{abs}$ and $\bar{\nu}_{em}$ *vs.* the dielectric constant, ε (A and B), and $f(n^2)$ (C and D) for the BODIPY derivatives **2-Ethyn** (■), **3-Ethyn** (🟥), **8-Ethyn** (🟦), and **3-Styryl** (■).

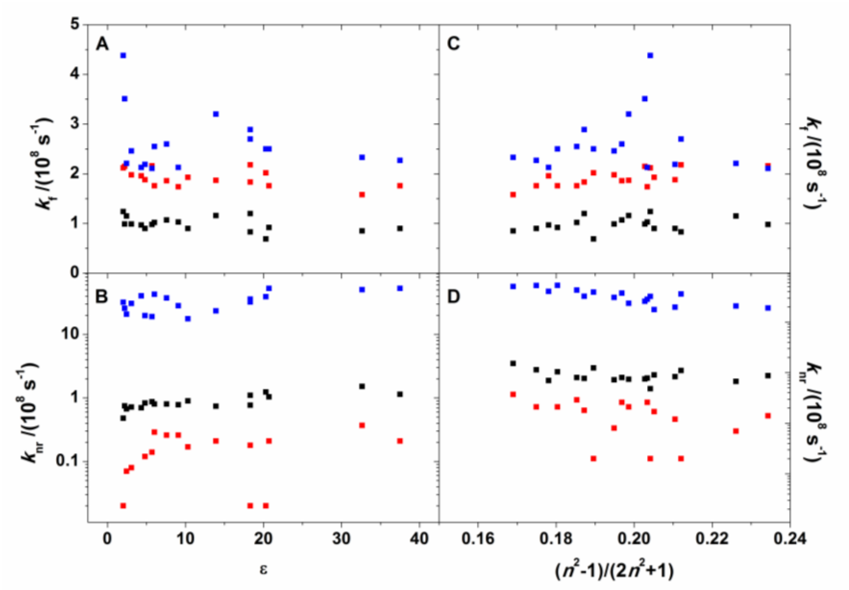

Figure S13. Correlations of k_f and k_{nr} *vs.* the dielectric constant, ε (A and B), and $f(n^2)$ (C and D) for the BODIPY derivatives **2-Ph** (■), **3-Ph** (🟥), and **8-Ph** (🟦).

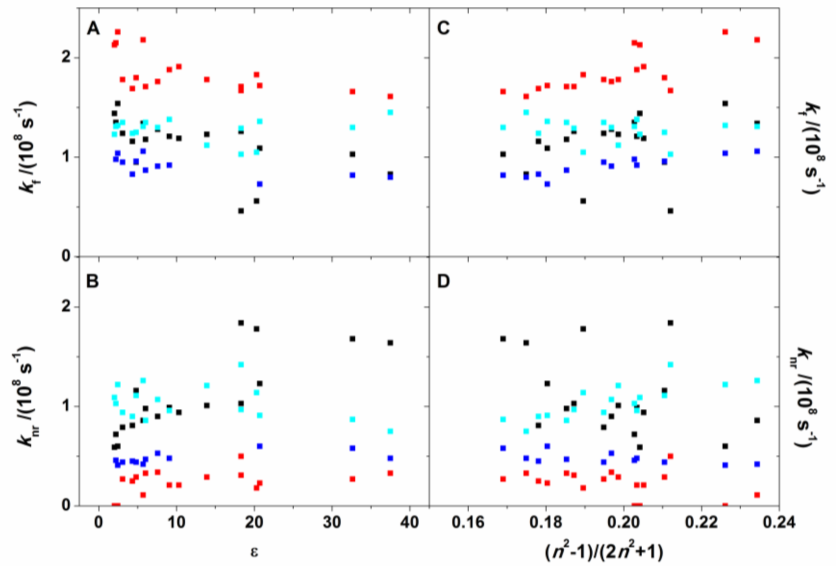

Figure S14. Correlations of k_f and k_{nr} *vs.* the dielectric constant, ε (A and B), and $f(n^2)$ (C and D) for the BODIPY derivatives **2-Ethyn** (■), **3-Ethyn** (🟥), **8-Ethyn** (🟦), and **3-Styryl** (■).

ESI References

1. N. Boens, L. Wang, V. Leen, P. Yuan, B. Verbelen, W. Dehaen, M. Van der Auweraer, W. D. De Borggraeve, L. Van Meervelt, J. Jacobs, D. Beljonne, C. Tonnelé, R. Lazzaroni, M. J. Ruedas-Rama, A. Orte, L. Crovetto, E. M. Talavera and J. M. Alvarez-Pez, *J. Phys. Chem. A*, 2014, **118**, 1576-1594.
2. J. Catalán, *J. Phys. Chem. B*, 2009, **113**, 5951-5960.